Fluctuation analysis of the surface microrelief of silicon-on-insulator structures after radiation exposure *

© A.S. Puzanov[1,2], I.Yu. Zabavichev[1,2], N.D. Abrosimova[1], V.V. Bibikova[1,2], E.V. Volkova[2], A.D. Nedoshivina[2], A.A. Potekhin[1,2], E.A. Tarasova[2], S.V. Hazanova[2], B.A. Loginov[3], D.Yu. Blinnikov[4], V.S. Vtorova[4], V.V. Kirillova[4], E.A. Liashko[4], V.S. Makeev[4], A.R. Pervykh[4], S.V. Obolensky[2,1]

[1] Russian Federal Nuclear Center — All-Russian Scientific Research Institute of Experimental Physics, 607188 Sarov, Nizhny Novgorod region, Russia
[2] Lobachevski University of Nizhny Novgorod, 603950 Nizhny Novgorod, Russia
[3] National Research University of Electronic Technology (MIET), 124498 Zelenograd, Russia
[4] Edication Center „Sirius“, 354349 Sochi, Russia

E-mail: puzanov@rf.unn.ru

Received January 20, 2025
Revised January 21, 2025
Accepted January 21, 2025

Using the method of two-dimensional fluctuation analysis, images of the surface of „silicon on insulator“ structures were analyzed. It is found that the Hurst parameter of the non-irradiated surface was $H_0 = 0.93$, for γ-ray irradiation $H_\gamma = 0.71-0.87$ and for neutron irradiation $H_n = 0.91-0.94$. This indicates that non-power correlations of the height function and random walk type processes for all the samples studied. The influence of radiation on the change in the standarddeviation and correlation length of the microroughness of the surface of samples at the microscale and the degradation.

Keywords: silicon on insulator, micro-roughness, charge carrier mobility, fluctuation analysis, fractal dimension.

DOI: 10.61011/SC.2024.12.60384.7548

1. Introduction

Surface and layer interface micro-roughness is an important process parameter characterizing the quality and electrophysical performance of semiconductor structures. The influence of the surface on the mobility of charge carriers using germanium as an example was first discussed in [1] and generalized in [2]. The importance of this effect for quantum wells with characteristic thicknesses of the order of the free path length of charge carriers and less is shown. When the thickness of the quantum well is reduced to the scale of the electron or hole wavelength, the quantization effect begins to appear. In this case, the change in the profile of the quantum well in different sections along the channel of the transistor due to fluctuations in its thickness leads to the emergence of an additional mechanism of charge carriers scattering, which also leads to a decrease in their mobility, as was found in [3]. A similar reduction in mobility can be achieved by splitting the levels at weak [4] and strong [5] magnetic field.

The development of technology for manufacturing field-effect transistors based on metal-oxide-semiconductor structures, on the one hand, made research into the influence of micro-roughness of interfaces on the electrophysical characteristics of semiconductor devices more relevant, and on the other hand it facilitated obtaining high-quality samples, which led to a series of application-oriented studies [6–14] related to bulk silicon structures.

Similarly, the emergence of field-effect transistors with high electron mobility [15] and the family of silicon-on-insulator [16] technologies has urged the analysis of the effect of micro-roughness on the behavior of quantum-sized [17] and thin-film [18] semiconductor elements. Currently, the calculation of charge carrier transport in transistor structures, taking micro-roughness into account, is mainly carried out ab initio by numerical methods [19]. An important issue in this case is not only the numerical value of the standard deviation Δ and correlation length Λ of the micro-roughness, but also the very kind of its autocorrelation function [20]. Indeed, according to the theoretical model set forth, for example, in the monograph [21], the rate of charge carrier transitions $S(p, p')$ from the state with momentum p to the state with momentum p' at scattering on micro-roughness is described by the expression

$$S(p, p') = \frac{2\pi}{\hbar} (qE_{\text{eff}})^2 |S(\beta)|^2 \delta(E' - E), \qquad (1)$$

where $\hbar$ — Planck constant, q — electron charge, E_{eff} — longitudinal boundary electric field strength, $S(\beta)$ — spectral power density as a function of spatial frequency β, which is related to the autocorrelation function via Fourier

* XXVIII International Symposium „Nanophysics and Nanoelectronics“, Nizhny Novgorod, March 11–15, 2024.

transform. This leads to a theoretical dependence of the mobility μ on the standard deviation and correlation length of the micro-roughness of type

$$\mu \sim \frac{1}{\Delta^2 \Lambda^2}. \quad (2)$$

An important factor affecting the profile of the potential well forming the channel of a field-effect transistor is the bound charge on the surface or layer interface. In [22] a simple analytical formula has been proposed based on theoretical representations and generalization of experimental data, which relates the mobility of charge carriers in the silicon layer $(\mu, \mathrm{cm}^2/(\mathrm{V}\cdot\mathrm{s}))$ to the concentrations of bound charge (Q_f, cm^{-2}) and impurity atoms (N_A, cm^{-3})

$$\mu = \frac{\mu_0(N_A)}{1 + f(N_A)Q_f},$$

$$\mu_0(N_A) = 3490 - 164 \cdot \log N_A,$$

$$f(N_A) = -0.104 + 0.0193 \cdot \log N_A. \quad (3)$$

In [23], the formula (3) was generalized to the case of radiation exposure. In this model, the concentration of bound charge is determined by the absorbed dose of ionizing radiation.

The fractal dimensionality of radiation defect clusters in the channels of GaAs Schottky field-effect transistors after exposure to the instantaneous neutron flux of the fission spectrum has been theoretically investigated. The development of nondestructive methods of surface investigation, first of all atomic force microscopy, allowed to experimentally find numerical values of the standard deviation and correlation length of micro-roughness of the investigated samples [25]. The emergence of fractal geometry [26] raised the question of the fractal dimensionality of the standard deviation and correlation length of micro-roughness [27], as well as the insufficiency of their point estimates for calculating the charge carrier mobility. Using fluctuation analysis [28] to analyze the correlation properties of the surface [29,30] opens up new opportunities to search for local disturbances introduced by radiation exposure [31–33] against the background of natural surface micro-roughness before irradiation. Note that an important advantage of fluctuation analysis over alternative approaches of statistical analysis of the surface as a random process is the possibility to describe and classify the structural complexity of the surface taking into account the spatial scale, since the sizes of radiation disturbances of the surface vary from fractions (individual point defects at γ-irradiation) to tens of nanometers (clusters of radiation defects at irradiation by the flux of instantaneous neutrons of the fission spectrum).

2. Objects and Methods of Experimental Investigations

In this paper a fluctuation analysis of the correlation properties of the surface of silicon-on-insulator structures before and after exposure to pulsed γ- and γ-neutron radiation, as well as their influence on the degradation of charge carrier mobility in the silicon layer after radiation exposure was carried out. Surface correlation properties were determined from analyzing images obtained with an atomic force microscope [34] at a resolution of 3.2 nm.

The silicon device layer and the hidden dielectric of the studied silicon-on-insulator structures had the same thickness of 200 nm, the substrate and the device layer had p-type conductivity and crystal-lattice orientation $\langle 100 \rangle$. The hole mobility was determined from the volt-ampere characteristics obtained by the pseudo-MDT transistor method using a mercury probe [35] electrophysical parameter measurement system, and were $\mu_0 = 250\,\mathrm{cm}^2/(\mathrm{V}\cdot\mathrm{s})$ before irradiation, $\mu_\gamma = 34{-}60\,\mathrm{cm}^2/(\mathrm{V}\cdot\mathrm{s})$ after γ-irradiation, and $\mu_n = 30{-}90\,\mathrm{cm}^2/(\mathrm{V}\cdot\mathrm{s})$ after neutron irradiation.

As noted in [33], irradiation of the samples leads to significant development of micro-roughness on the surface of silicon-on-insulator structures. Under neutron irradiation, larger-scale structures are formed than under γ-irradiation due to the higher initial energy of the primary recoil atoms. However, the number of primary recoil atoms is higher under γ-irradiation, which leads to a locally „rugged“ surface. Note that the degree of „ruggedness“ of a stationary random process is determined by the Hurst parameter H $(0 < H < 1)$ [36], while for a nonstationary — the scale index of the fluctuation function α. For a stationary random process, the scale index of the fluctuation function and the Hurst parameter coincide $(H \equiv \alpha)$ while for a nonstationary one they differ by one $(H \equiv \alpha - 1)$. At small values of the Hirst parameter the random process has a high ripple, at high values — the ripple is smoother, which is due to the ppersistence property (preservation of the existing trend) at $H > 0.5$ and antipersistence at $H < 0.5$. In addition, the Hurst parameter is related to the aforementioned fractal dimension of radiation disturbances D as $H \equiv D - 2$. Thus, it is of interest to quantitatively analyze the changes in surface micro-roughness of samples of silicon-on-insulator structures after radiation exposure, taking into account the Hurst parameter and its generalizing indicator of the scale of the fluctuation function.

3. Calculation procedure

There are variations of the fluctuation analysis method for the two-dimensional case, so makes sense to consider the calculation methodology in detail.

At the first stage of calculations the cumulative surface of the form

$$Y_{i,j} = \sum_{n=1}^{i \le N} \sum_{m=1}^{j \le M} h_{n,m}, \quad (4)$$

where h — the height matrix of size $N \times M$.

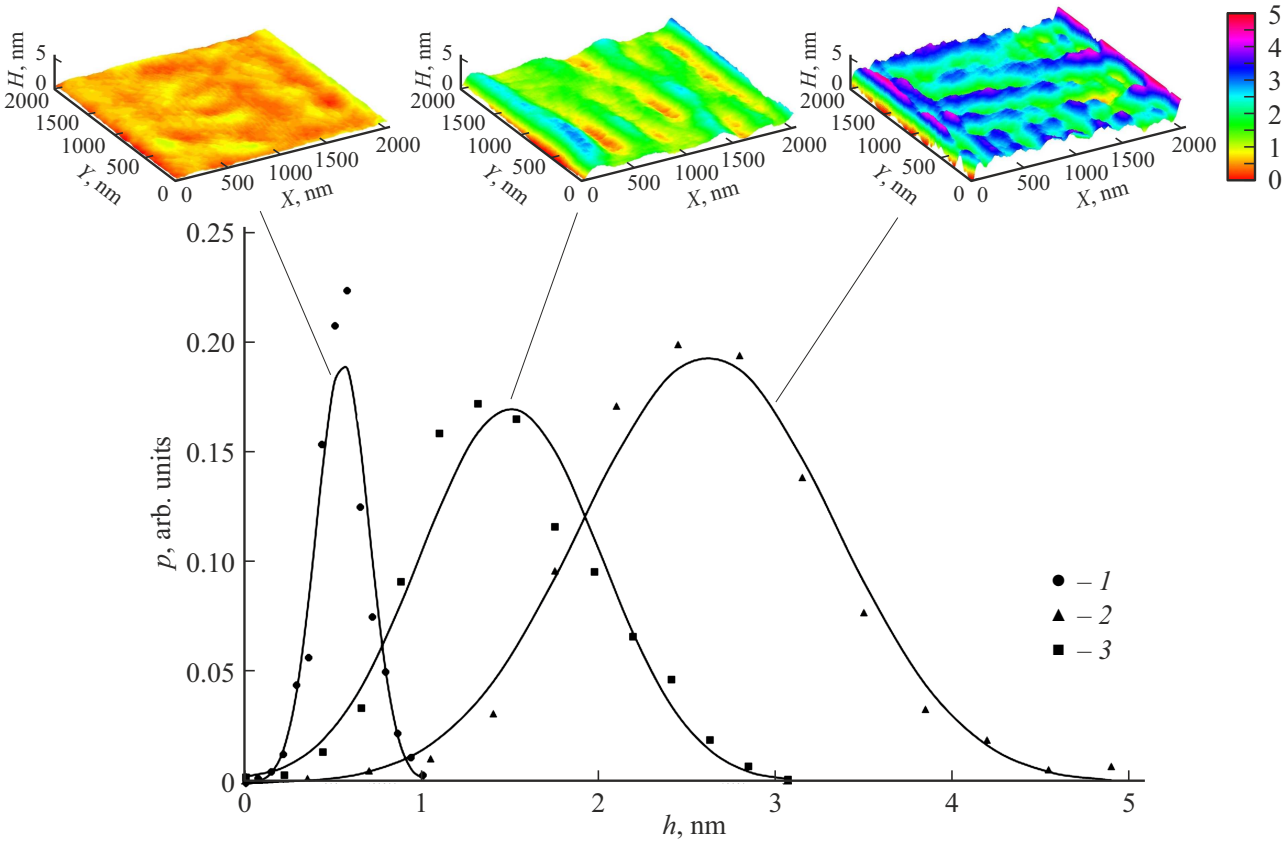

Figure 1. The surface height distribution functions of the samples are: *1* — before irradiation, *2* — after γ-irradiation, *3* — after neutron irradiation; solid curves — approximating normal distribution. The inset shows the microrelief of the samples (from left to right): before irradiation, after neutron irradiation, and after γ-irradiation.

At the second stage, the cumulative surface was divided into non-intersecting square segments of size $s \times s$, and then a trend function subtraction procedure was applied to each segment, minimizing the residual function of each segment:

$$\varepsilon_{u,w,i,j} = Y_{u,w,i,j} - \tilde{Y}_{u,w,i,j}, \tag{5}$$

where $Y_{u,w}$ — a segment of the cumulative function, $\tilde{Y}_{u,w,i,j}$ — its trend function.

It can be shown that regardless of the type of trend function, the following condition must be satisfied

$$\langle \varepsilon_{u,w} \rangle = 0. \tag{6}$$

At the third stage, the standard deviations of the residual function were calculated for each segment as a function of its size:

$$F_{u,w}(s) = \sqrt{\langle \varepsilon_{u,w}^2 \rangle}. \tag{7}$$

The fluctuation function is found as the average of the standard deviations of the residuals functions of all segments of the cumulative surface:

$$F(s) = \langle F_{u,w}(s) \rangle \propto s^{\alpha}. \tag{8}$$

Table 1. Point estimates of the mean values and standard deviations of the surface height of the samples

Parameter	Sample		
	Before irradiation	After γ-neutron	After irradiation
Average value, nm	0.547	2.612	1.496
RMS deviation, nm	0.148	0.711	0.508

The simplest trend function is a horizontal plane whose height is the mean of the segment of the cumulative function, which is a generalization of Hurst's method to the two-dimensional case for a stationary random process. For the two-dimensional nonstationary random process, the trend plane is inclined along both coordinates [37], which leads to a mismatch of the scale index with the known scale for the one-dimensional case. To solve this problem, a method of line-by-line or column-by-column trend compensation that preserves the scale of the scale index is proposed in [29,30]. The disadvantage of this approach is that it ignores the correlation of heights between columns in line-by-line compensation or the correlation of

Table 2. Values of the scale index of the fluctuation function of the surface micro-roughness of the samples. The square of the Pearson correlation coefficient is shown in brackets

Calculation method	Sample		
	before irradiation	After γ-irradiation	After neutron irradiation
Hurst method*	0.926 ($R^2 = 0.995$)	0.870 ($R^2 = 0.990$)	0.944 ($R^2 = 0.995$)
Plane Campbell's method with axes OX and OY compensation	1.910 ($R^2 = 0.993$)	1.740 ($R^2 = 0.983$)	1.896 ($R^2 = 0.993$)
Plane Campbell's method with axis OX compensation	1.161 ($R^2 = 0.997$)	1.051 ($R^2 = 0.995$)	1.384 ($R^2 = 0.995$)
Plane Campbell's method with axis OY compensation	0.950 ($R^2 = 0.996$)	0.890 ($R^2 = 0.994$)	0.947 ($R^2 = 0.995$)
Line-by-line trend compensation Campbell's method	1.892 ($R^2 = 0.995$)	1.963 ($R^2 = 0.996$)	1.551 ($R^2 = 0.995$)
Line-by-line trend compensation Campbell's method	1.926 ($R^2 = 0.992$)	1.705 ($R^2 = 0.977$)	1.911 ($R^2 = 0.993$)

Note. * For a non-stationary random process, the value of the scale index in the Hurst method is one less than that of the line-by-line and column-by-column Campbell's method.

Table 3. Values of the scale index of the standard deviation of the surface micro-roughness of the samples. The square of the Pearson correlation coefficient is shown in brackets.

Calculation method	Sample		
	before irradiation	After γ-irradiation	After neutron irradiation
Hurst method	0.726 ($R^2 = 0.981$)	0.728 ($R^2 = 0.977$)	0.780 ($R^2 = 0.988$)
Plane Campbell's method with axes OX and OY compensation	0.940 ($R^2 = 0.965$)	1.040 ($R^2 = 0.992$)	0.983 ($R^2 = 0.985$)
Plane Campbell's method with axis OX compensation	0.796 ($R^2 = 0.984$)	0.888 ($R^2 = 0.981$)	0.822 ($R^2 = 0.982$)
Plane Campbell's method with axis OY compensation	0.769 ($R^2 = 0.985$)	0.742 ($R^2 = 0.981$)	0.828 ($R^2 = 0.986$)
Line-by-line trend compensation Campbell's method	1.041 ($R^2 = 0.966$)	1.015 ($R^2 = 0.986$)	0.747 ($R^2 = 0.922$)
Line-by-line trend compensation Campbell's method	1.032 ($R^2 = 0.959$)	1.108 ($R^2 = 0.980$)	1.138 ($R^2 = 0.986$)

heights between rows in column-by-column trend compensation.

4. Results and discussion

At the preparatory stage of the calculations we analyzed the surface height distribution functions of the samples (Figure 1); the inset shows the microrelief of the samples before irradiation, after neutron irradiation and after γ-irradiation. The regions considered are typical for the wafer as a whole. It can be seen that the experimental results are well described by a normal distribution, the parameters of which are given in Table 1. Although fluctuation analysis can be used to analyze random processes with arbitrary statistics, the use of models relating the mobility of charge carriers to the spectral power density or the autocorrelation function of micro-roughness implicitly requires a near-Gaussian random process, since it is fully described by its second statistical moment and ignores higher order statistical moments.

The results of calculating the fluctuation function for the samples of silicon-on-insulator [33] structures are shown in Figure 2, the values of the scale parameter for different versions of the procedure of subtracting the average value of the cumulative surface segments are given in Table 2. For all the studied samples, regardless of the applied

Table 4. Values of the scale index of the correlation length of the micro-roughness of the sample surface in the exponential (top row) and Gaussian (bottom row) approximations. The square of the Pearson correlation coefficient is shown in brackets.

Calculation method	Sample		
	Before irradiation	After γ-irradiation	After neutron irradiation
Hurst method	0.846 ($R^2 = 0.995$) 8.880 ($R^2 = 0.996$)	0.830 ($R^2 = 0.998$) 0.839 ($R^2 = 0.999$)	0.897 ($R^2 = 0.998$) 0.912 ($R^2 = 0.998$)
Plane Campbell's method with axes *OX* and *OY* compensation		0.9823 ($R^2 = 0.999$) 0.9807 ($R^2 = 0.999$)	
Plane Campbell's method with axis *OX* compensation	0.789 ($R^2 = 0.986$) 0.823 ($R^2 = 0.992$)	0.848 ($R^2 = 0.995$) 0.860 ($R^2 = 0.997$)	0.836 ($R^2 = 0.978$) 0.866 ($R^2 = 0, 985$)
Plane Campbell's method with axis *OY* compensation	0.824 ($R^2 = 0.991$) 0.857 ($R^2 = 0.994$)	0.821 ($R^2 = 0.997$) 0.832 ($R^2 = 0.998$)	0.904 ($R^2 = 0.997$) 0.922 ($R^2 = 0.998$)
Line-by-line trend compensation Campbell's method		0.980 ($R^2 = 0.999$) 0.981 ($R^2 = 0.999$)	
Line-by-line trend compensation Campbell's method		0.968 ($R^2 = 0.998$) 0.957 ($R^2 = 0.998$)	

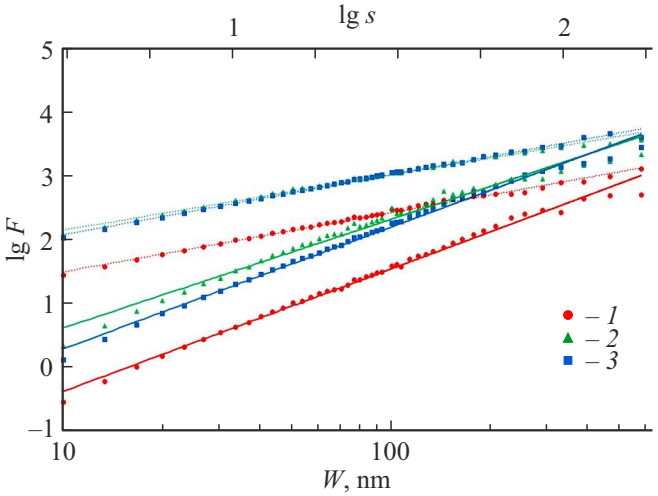

Figure 2. The fluctuation function of surface micro-roughness of the samples as a function of segment size: dotted line — Hurst method; solid line — line-by-line fluctuation trend compensation method; *1* — before irradiation, *2* — after γ-irradiation, *3* — after neutron irradiation.

algorithm of subtracting the average value of the cumulative surface segments, there is a linear dependence of the fluctuation function on the scale parameter in the log-log scale, which indicates monofractality. Thus, the insensitivity of the method to the clusters of radiation defects appearing after radiation exposure is apparently explained by their stochastic distribution in size and position on the surface of irradiated samples, which „blurs“ a small break at the beginning of the curves.

The Hurst method and the column-by-column trend compensation Campbell's method give close values of the Hurst parameter, which for the unirradiated surface is $H_0 = 0.93$, irradiated by γ-quanta $H_\gamma = 0.71-0.87$ irradiated by neutrons $H_n = 0.91-0.94$, indicating non-degenerate correlations of the height function and processes of the random walk type for all the studied samples. Apparently, the obtained result is due to the discreteness of the surface height map both at the physical level (self-similarity cannot continue at scales smaller than the interatomic distances) and at the level of the initial data of the mathematical algorithm due to the spatial resolution of the atomic force microscope probe. In this case, the difference from most

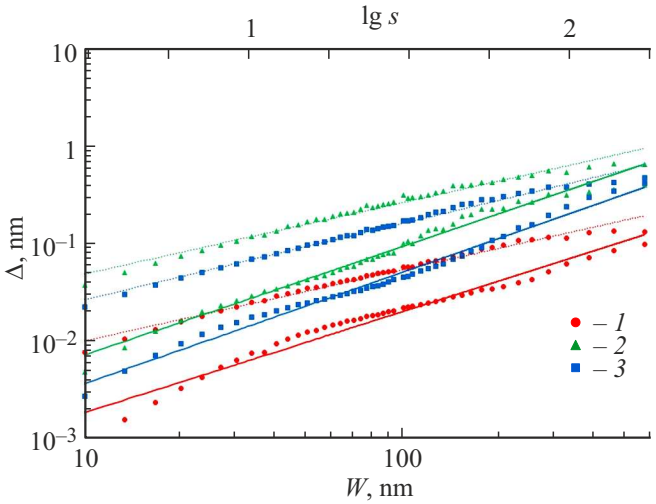

Figure 3. RMS deviation of surface micro-roughness of samples as a function of segment size: dotted line — Hurst method, solid line — line-by-line fluctuation trend compensation method; *1* — before irradiation, *2* — after γ irradiation, *3* — after neutron irradiation.

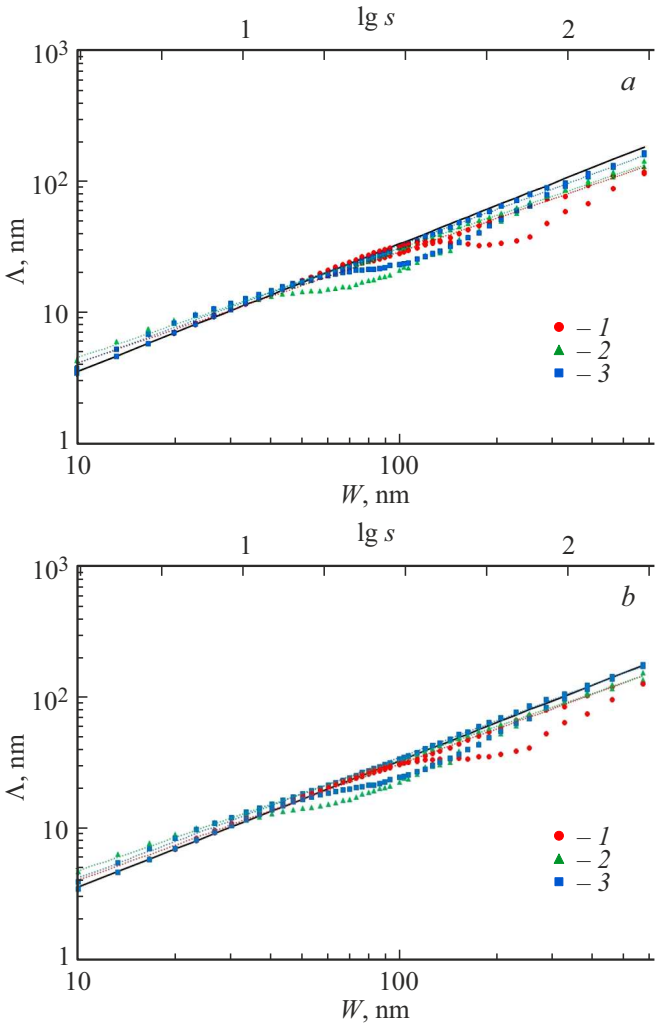

Figure 4. Correlation length of surface micro-roughness of samples as a function of segment size: dotted line — Hurst method, solid line — line-by-line fluctuation trend compensation method; *1* — before irradiation, *2* — after γ-irradiation, *3* — after neutron irradiation; *a* — in exponential approximation, *b* — in Gaussian approximation of autocorrelation function.

self-similar natural processes is the larger value of the Hurst parameter, which is usually in the range of 0.72–0.73 [38]. This indicates a smoother change in the surface height of the unirradiated sample compared to „natural" micro-roughness, which is due to technological processing, as well as irradiated by the instantaneous neutron flux of the fission spectrum due to radiation annealing. On the contrary, the micro-roughness of the sample after γ-irradiation tends to the natural value, which is explained by insufficient energy of primary γ primary atoms for significant radiation annealing. The line-by-line Campbell's method of trend compensation gives significantly different values of the scale exponent of the fluctuation function from those presented above, which is due to the direction of the fast scanning axis of the atomic force microscope implemented during the experiments.

As noted above, the values of the scale index for the Campbell's method in the plane with trend compensation in one or both axes are irreducible to the Hurst parameter. Nevertheless, it can be observed that the values of the scale index for the Campbell's method on the plane with trend compensation on both axes are close to the values obtained above at $H \approx \alpha_{xy} - 1$, and for the Campbell's method on the plane with trend compensation on axis OY — at $H \approx \alpha_y$.

In order to estimate the RMS deviation of the surface micro-roughness of the samples (Figure 3, Table 3), the height matrix was directly subjected to the segmentation procedure and subtraction of the mean value. It can be seen that the RMS deviation of surface micro-roughness increases after radiation exposure, which is one of the mechanisms of charge carriers mobility decrease in the silicon layer of silicon-on-insulator structures after irradiation. Note that the point estimates of the RMS deviation of micro-roughness of the samples given in Table 1 are the limit for the whole surface ($W = 2303.3$ nm, $\lg(s) = 2.84$).

Unlike the standard deviation, the correlation length of the micro-roughness surface of the samples (Figure 4, Table 4) changes little after irradiation. The correlation length of surface micro-roughness of each segment was found by least-square method for exponential and Gaussian functions. The calculation results were confirmed to be correct by comparison with data obtained using open-source software [39] for the complete surface.

The results of measuring the hole mobility in the samples of "silicon-on-insulator„ structures before and after irradiation show the presence of correlation (the square of Pearson correlation coefficient varies in the range $R^2 = 0.922–0.993$) with the root-mean-square deviation of micro-roughness (Figure 5) with the degree exponent in the range $\beta = -(1.214–1.048)$ depending on the segment size. The difference from the theoretical dependence $\beta = -2$ according to expression (2) seems to be due to additional charge carrier scattering mechanisms playing an important role at normal temperature of the samples.

5. Conclusion

The calculation results show the influence of irradiation on the correlation properties of the surface micro-roughness of silicon-on-insulator samples. The appearance of an additional scattering mechanism predictably reduces the mobility of charge carriers, but the obtained index of the degree of calculation-experimental dependence differs from the theoretical value, which is due to the influence of additional scattering mechanisms, manifested at normal temperature of the samples. The obtained results show the importance of taking into account the non-ideality of layer interfaces when modeling the charge carrier transport in bulk, quantum-dimensional and thin-film structures subjected to irradiation, and can serve as initial data for

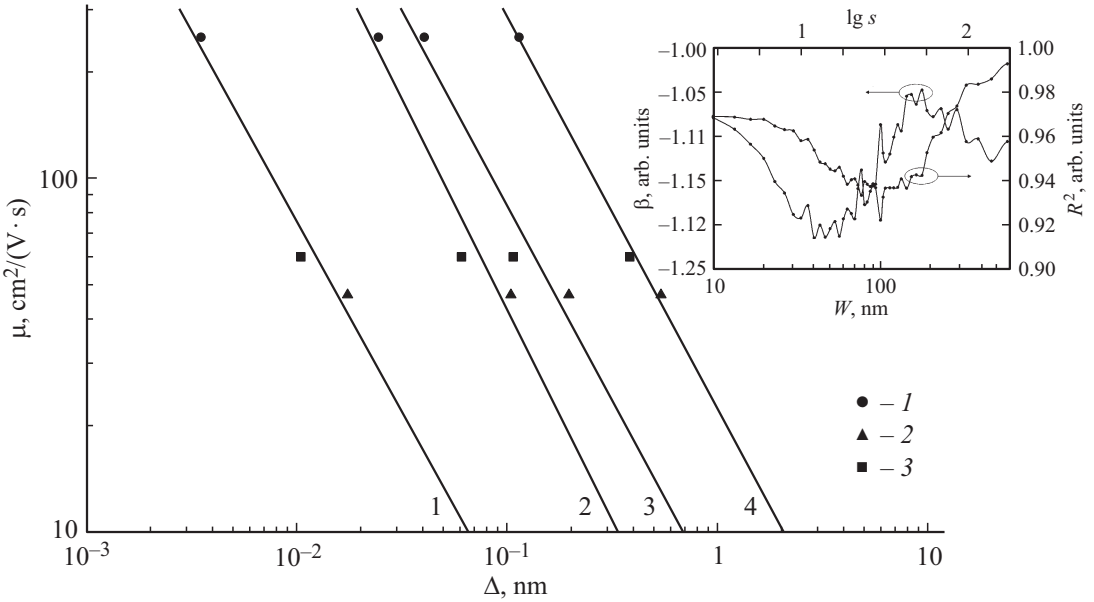

Figure 5. Hole mobility in the silicon layer of the silicon-on-insulator structure as a function of the standard deviation of the micro-roughness of the samples: *1* — before irradiation, *2* — after γ-rradiation, *3* — after neutron irradiation at different segment sizes: 1 — 10×10 nm, 2 — 60×60 nm, 3 — 120×120 nm, 4 — 573×573 nm. The inset shows the dependence of the approximation degree index and the square of the Pearson correlation coefficient on the segment size.

numerical models of semiconductor elements with complex consideration of radiation effects and micro-roughness.

Funding

The study was funded by the Ministry of Science and Higher Education of the Russian Federation under the state order of N.I. Lobachevsky Nizhny Novgorod State University (FSWR-2024-0003).

Conflict of interest

The authors declare that they have no conflict of interest.

References

[1] J.R. Schriepper. Phys. Rev., **97** (3), 641 (1955).
[2] R.F. Greene, D.R. Frankl, J. Zemel. Phys. Rev., **118** (4), 967 (1960).
[3] F. Stern, W.E. Howard. Phys. Rev., **163** (3), 816 (1967).
[4] R.E. Prange, T.-W. Nee. Phys. Rev., **168** (3), 779 (1968).
[5] T. Ando. J. Phys. Soc. Japan, **43** (5), 1616 (1977).
[6] R.F. Pierret, C.T. Sah. Solid-State Electron., **11**, 279 (1968).
[7] C.T. Sah, T.H. Ning, L.L. Tschopp. Surf. Sci., **32**, 561 (1972).
[8] Y.C. Cheng, E.A. Sullivan. Surf. Sci., **34**, 717 (1973).
[9] Y.C. Cheng, E.A. Sullivan. J. Appl. Phys., **44** (8), 3619 (1973).
[10] Y.C. Cheng, E.A. Sullivan. J. Appl. Phys., **45** (1), 187 (1974).
[11] Y. Matsumoto, Y. Uemura. Jpn. J. Appl. Phys., **2**, 367 (1974).
[12] J.R. Brews. J. Appl. Phys., **46** (5), 2193 (1975).
[13] A. Hartstein, T.H. Ning, A.B. Fowler. Surf. Sci., **58**, 178 (1976).
[14] F. Stern. Phys. Rev. Lett., **44** (22), 1469 (1980).
[15] T. Mimura. IEEE Trans. Microw. Theory Tech., **50** (3), 780 (2002).
[16] G.K. Celler, S. Cristoloveanu. J. Appl. Phys., **93** (9), 4955 (2003).
[17] H. Sakaki, T. Noda, K. Hirakawa, M. Tanaka, T. Matsusue. J. Appl. Phys., **51** (23), 1934 (1987).
[18] K. Uchida, S.-I. Takagi. J. Appl. Phys., **82** (17), 2916 (2003).
[19] A. Pirovano, A.L. Lacaita, G. Zandler, R. Oberhuber. IEEE Trans. Electron Dev., **47** (4), 718 (2000).
[20] A. Pirovano, A.L. Lacaita, G. Ghidini, G. Tallarida. IEEE Electron Dev. Lett., **21** (1), 34 (2000).
[21] M. Lundstrom. *Fundamentals of carrier transport* (Cambridge University Press, 2000).
[22] S.C. Sun, J.D. Plummer. IEEE Trans. Electron Dev., **27** (8), 1497 (1980).
[23] F.W. Sexton, J.R. Schwank. IEEE Trans. Nucl. Sci., **32** (6), 3975 (1985).
[24] E.V. Kiseleva, S.V. Obolensky. Mikroelektronika, **35** (5), 374 (2006). (in Russian).
[25] S.M. Goodnick, D.K. Ferry, C.W. Wilmsen, Z. Liliental, D. Pathy, O.L. Krivanek. Phys. Rev. B, **32** (12), 8171 (1985).
[26] B.B. Mandelbrot. *The Fractal Geometry of Nature* (N.Y., Freeman, 1982).
[27] T. Yoshinobu, A. Iwamoto, H. Iwasaki. Jpn. J. Appl. Phys., **33** (1A), 67 (1994).
[28] C.-K. Peng, S. Havlin, H.E. Stanley, A.L. Goldberger. Chaos, **5**, 82 (1995).
[29] A.V. Alpatov, S.P. Vikhrov, N.V. Grishankina. FTP, **47** (3), 340 (2013). (in Russian).
[30] A.V. Alpatov, S.P. Vikhrov, N.V. Rybina. FTP, **49** (4), 467 (2015). (in Russian).
[31] S.V. Obolenskii, E.V. Volkova, A.B. Loginov, B.A. Loginov, E.A. Tarasova, A.S. Puzanov, S.A. Korolev. Pis'ma ZhTF, **47** (5), 38 (2021). (in Russian).

[32] E.V. Volkova, A.B. Loginov, B.A. Loginov, E.A. Tarasova, A.S. Puzanov, S.A. Korolev, E.S. Semenovykh, S.V. Khazanova, S.V. Obolensky. FTP, **55** (10), 846 (2021). (in Russian).
[33] B.A. Loginov, D.Yu. Blinnikov, V.C. Vtorova, V.V. Kirillova, E.A. Lyashko, V.S. Makeev, A.R. Pervykh, N.D. Abrosimova, I.Yu. Zabavichev, A.S. Puzanov, E.V. Volkova, E.A. Tarasova, S.V. Obolensky. ZhTF, **93** (7), 1025 (2023). (in Russian).
[34] B.A. Loginov, P.B. Loginov, V.B. Loginov, A.B. Loginov. Nanoindustriya, **12** (6), 352 (2019). (in Russian).
[35] D.K. Schroder. *Semiconductor Material and Device Characterization* (N.J., Wiley-IEEE Press, 2006).
[36] H.E. Hurst. Trans. Am. Soc. Civil Eng., **116**, 770 (1951).
[37] A.-L. Barabasi, H.E. Stanley. *Fractal concepts in surface growth* (Cambridge, Cambridge University Press, 1995).
[38] Yu.A. Kalush, V.M. Loginov. Sib. journ. industr. matem, **5** (4), 29 (2002). (in Russian).
[39] D. Necas, P. Klapetek. Cent. Eur. J. Phys., **10** (1), 181 (2012).

Translated by J.Savelyeva